MODELING OF THE EFFECTS OF LATERAL VELOCITY VARIATIONS ON SEISMIC DATA USING THE WAVE EQUATION

HANS J. TIEMAN[1]

ABSTRACT

An alternative solution to the wave equation is derived, and used as a basis for development of a seismic modeling program written specifically to investigate the effects of lateral velocity variations on the appearance of seismic data. This solution is obtained by splitting the wavefield into its upcoming and downgoing components after having replaced the wave equation with an integral form. Dividing the velocity field into X-independent and X-dependent components results in an optimum approximation to the solution, one that is both accurate, and applicable over relatively large extrapolation steps.

Results of the modeling system confirm that structures and amplitude variations on a reflection event result from two contrasting causes, one associated with reflection and the other with refraction. The latter process can produce all the features normally associated with reflection from complex regions. These features include vertical and horizontal displacement of reflector position, and amplitude variations, both of which have no correspondence with actual reflector structure or strength.

INTRODUCTION

Wave-theory techniques used in exploration geophysics have not always adequately accounted for all the effects of subsurface inhomogeneities on the appearance of seismic data. Through the process of reflection or refraction, inhomogeneities are directly responsible for all the structural and amplitude variations on reflection events. Refraction effects, produced when waves propagate through complex regions, are particularly difficult to handle with wave-theory techniques. They can produce all the features associated with reflection from complex regions, including vertical and horizontal displacement of reflector position, amplitude diminution or brightening, focusing or unfocusing of waves, and diffraction development. These effects not only tend to obscure the information contained by seismic waves about the reflectors that originated the waves, but can produce phantom structures and amplitude variations that have no correlation with actual reflector changes.

Recently, wave-equation techniques have been developed that can handle all these effects (for example, Judson et al., 1980 and Larner et al., 1980). The techniques developed by Judson and Larner can be derived from the wave equation by the introduction of a translating coordinate system with a frame velocity that has depth dependence but no lateral distance dependence. This procedure divides the wave equation into two components: a "thin lens" component consisting of the difference between the frame and material velocities, applied as a simple static shift, and a "wave" component that can be applied by using a finite-difference scheme. The two components applied recursively to a wavefield can continue it accurately through any complex region. Unfortunately, the theory is concerned only with the extrapolation of upcoming or downgoing wavefields; the term that couples the two wavefields at reflecting elements is not derived.

An exact solution to the scalar wave equation is proposed that completely accounts for all facets of wave propagation, including the term that controls the coupling of upcoming and downgoing wavefields. In principle, all the wave-theory techniques used at present in modeling or migration programs can be derived from this solution, with all the assumptions and approximations used in them explicitly

[1]Sefel Geophysical, 500 Bow Valley Square Two, Calgary, Alberta.

stated. With a physical interpretation of all the components in the solution, only those that are desired for a particular application need be used.

This paper has two objectives. One is to present the mathematical derivation of the proposed solution and the optimum approximation to it. The other is to use a modeling program, based on the optimum approximation, to investigate the effects of lateral velocity variations on seismic data.

THEORY

Wave theory allows one to construct a wavefield that is known for all points in space and time, given certain initial conditions and boundary values. Unfortunately, for either seismic migration or modeling, the classical wave equation is not set up in a fashion that would allow easy exploitation of the known initial conditions. Thus, there is a need for the mathematical manipulation of the wave equation to a form more amenable to seismic problems. The manipulations that follow are an extension of the work done by J. Claerbout (1971, 1976). The equations he developed have as their basic underlying assumption the stratified-earth model; the equations developed herein have no such assumption, and hold for any arbitrary velocity configuration in the earth's subsurface. Note that the resulting form of the equations derived is very similar to that deduced by Claerbout and others; however, the components of the vectors and matrices examined in this paper are complex operators that cannot be transformed by any straightforward means into simple numbers. The development that follows is given in much greater detail in the author's M.Sc. thesis (Tieman, 1980).

Equation 1, first published in this form by J. Claerbout (1971), is the starting point of the mathematical development.

$$\frac{d}{dz}\begin{bmatrix} P \\ W \end{bmatrix} = \begin{bmatrix} 0 & iA \\ iB & 0 \end{bmatrix}\begin{bmatrix} P \\ W \end{bmatrix} \tag{1}$$

where
P = pressure field
W = vertical velocity field
$A = \omega\rho$
ω = temporal frequency
ρ = mass density
$B = \dfrac{\omega}{K} - \dfrac{1}{\omega}\dfrac{\partial}{\partial x}\dfrac{1}{\rho}\dfrac{\partial}{\partial x}$

K = bulk modulus of rigidity

$\dfrac{\partial}{\partial x}$ = first derivative with respect to x (lateral distance)

Equation 1 is a differential formula describing the relationship between the pressure and velocity fields defined along two planes parallel to the earth's surface an infinitesimal distance apart. Note that a sinusoidal time dependence ($e^{-i\omega t}$) has been assumed for these fields (to be referred to collectively as wavefields). This allows for a separate consideration of any given frequency component of the fields. Operator notation (i.e., A, B in eq. 1) has been introduced both for brevity, and because it lends itself to the manipulations to be made. Note that the operators will in general be noncommuting; that is, the order of application to functions is very important*.

Equation 1 can be cast into an integral form by applying a Voltera Integral (Gantmakher, 1960), which results in the form given in equation 2†. (2)

$$\begin{bmatrix} P \\ W \end{bmatrix}_{z_N} = \lim_{\delta z \to 0} \left\{ e^{i\begin{bmatrix} 0 & A(z_N) \\ B(z_N) & 0 \end{bmatrix}\delta z} e^{i\begin{bmatrix} 0 & A(z_N-\delta z) \\ B(z_N-\delta z) & 0 \end{bmatrix}\delta z} \cdots e^{i\begin{bmatrix} 0 & A(z_0) \\ B(z_0) & 0 \end{bmatrix}\delta z} \right\} \begin{bmatrix} P \\ W \end{bmatrix}_{z_0}$$

---

*The assumption that operators can be manipulated as if they were simple numbers, although a meaningful concept, can introduce many pitfalls, especially if two or more noncommuting operators are involved. For instance, for any two noncommuting operators A and B, (where AB does not equal BA), exp(A + B) does not equal (expA) (expB), and $(AB)^{1/2}$ does not equal $A^{1/2}B^{1/2}$.

†Note that because the C(z) (equal to $\begin{bmatrix} 0 & A(z) \\ B(z) & 0 \end{bmatrix}$) operator is not self-commutative (that is $C(z_1)$ $C(z_2)$ does not equal $C(z_2)$ $C(z_1)$), the infinite product series cannot be transformed by the usual rule of exponential multiplication into an infinite summation series of the form given below:

$$\begin{bmatrix} P \\ W \end{bmatrix}_{z_n} = e^{i\int_{z_0}^{z_n}\begin{bmatrix} 0 & A \\ B & 0 \end{bmatrix}dz} \begin{bmatrix} P \\ W \end{bmatrix}_{z_0}$$

This is an important point that is missed by many authors.

subsurface configuration. Obviously the error in the approximation vanishes for the case where lateral velocity variations are negligible, if $\bar{v}$ is chosen to equal v.

Equation 13 was used by the author in the modeling program, the results of which follow. In implementation, the first term in equation 13 can be applied as a simple multiplication in the wave-number domain, the second as a multiplication in the spatial domain, and the last as either a short-term filter convolution, or a combination of multiplication in both domains.

MODELING EXAMPLES AND RESULTS

It should be emphasized that the following examples are assumed to be two-dimensional, with a source that is also two-dimensional. This may affect the rate at which diffractions and focused (or unfocused) reflections decay in amplitude. However, most seismic data are scaled in a time-variant manner during processing, which reduces the importance of this draw-

back. Because of the zero-offset assumption, multiple reflections and shear-wave conversions are not modeled.

The terms 'lens' will be used quite often in the following. It will have the same meaning as it has in optics, and will refer to any configuration that causes bending of wavefields, resulting in focusing or unfocusing as it is traversed. Obviously, in the real world, no perfect focusing or unfocusing lenses exist. Usually a perturbing region will combine both types of lens in varying degrees of complexity (see, for example, the faulted-anticline model).

The synthetic models presented in this paper are not meant to correspond to any existing or possible geological situation, but were chosen for their simplicity and in order to replicate some of the models studied by previous authors. Briefly, these models are composed of two surfaces: a curved upper surface, and a perfectly flat horizontal lower surface. The emphasis in
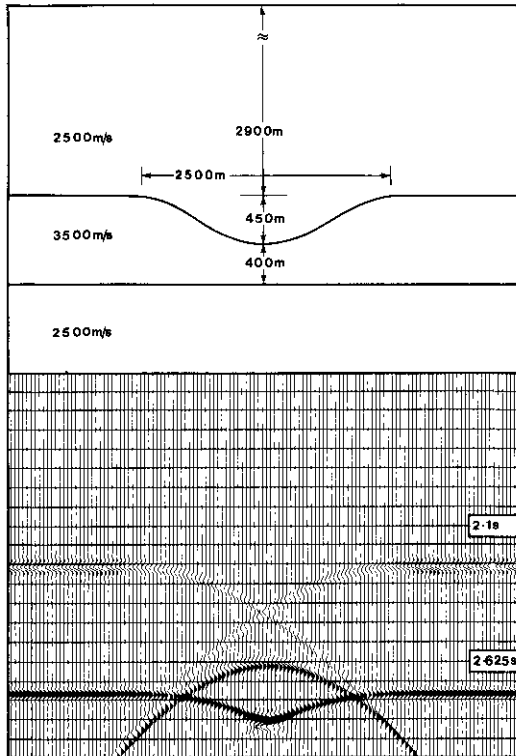

Fig. 1. Synform #1. The synformal feature in the upper surface of the Geological Model (upper figure), acts as a focusing lens on reflections from the lower region.
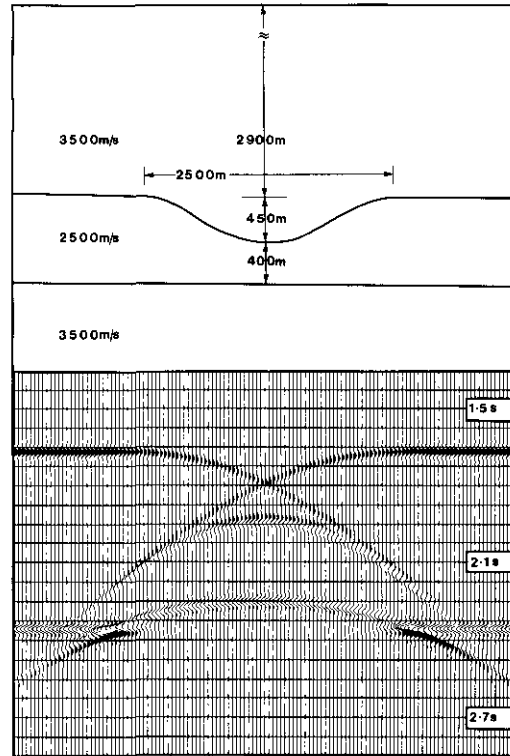

Fig. 2. Synform #2. The synform acts as a divergent lens on reflections from lower regions. Some ninety-degree phase shift and diffraction development is evident on both sides of the disturbed region.

this study will not be on the form of the reflection from the upper surface, since this is well understood and well presented in the literature (e.g., Hilterman, 1970), but on the perturbing effects the upper surfaces may have on waves emanating from the lower surfaces.

Figures 1 and 2 illustrate two synforms with the only difference between them being an interchange of velocities. In the example given in Figure 1, the synformal feature acts as a convergent lens, causing the focusing of any seismic waves that traverse the central region. This action results in the appearance of the perturbed seismic waves as a narrow band of high amplitude (in the centre of the profile at about 2.93 sec), slightly retarded in time relative to the unaffected waves (seen on either side at 2.82 sec). Note that between the focused high-amplitude band and the normal unperturbed waves, two regions of low amplitude exist.
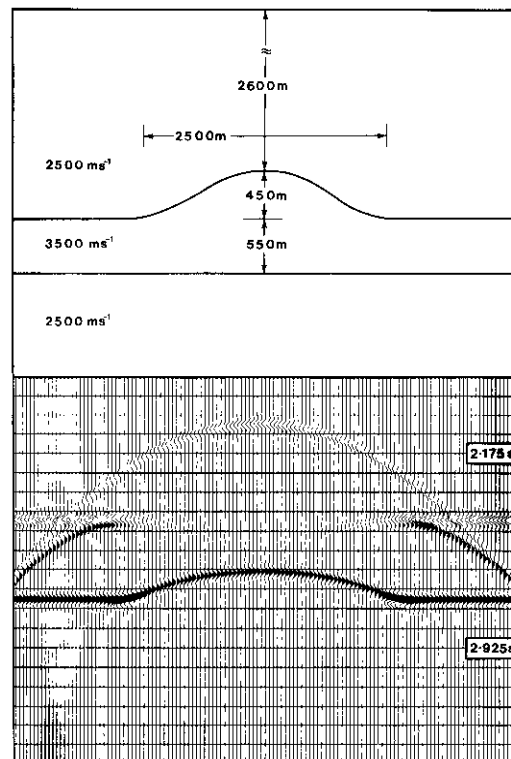
In the second example (Fig. 2), the synformal feature acts as a divergent lens, causing any seismic waves traversing this region to become unfocused. On the model record, this is shown by their arcuate form and lower amplitude (again situated in the centre of the profile, this time at about 2.25 sec). In this example these waves are advanced in time with respect to the unaffected seismic waves.

Analogous behaviour in the seismic response occurs in Figure 3 (divergence) and Figure 4 (convergence), each illustrating antiforms. Note that this time the velocity arrangement producing focusing effects is opposite in the antiformal case as compared with the synformal case. On examining both situations closely, it is evident that what causes a configuration to act as a focusing lens is its geometry, coupled with the lower-velocity composition of the lens compared with that of material laterally away from the lens. Figures 2 and 4 both
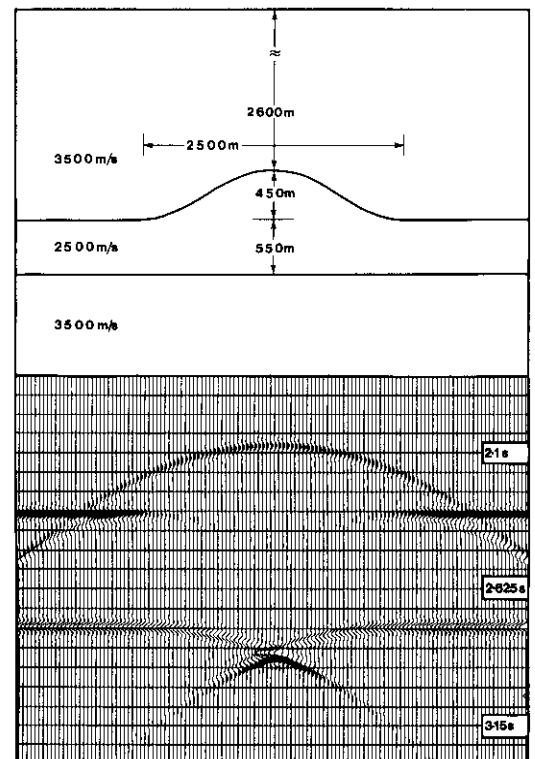

Fig. 3. Antiform #1. The antiform acts as a divergent lens on reflections from lower regions.

Fig. 4. Antiform #2. The antiform causes focusing of reflections from regions beneath it. Diffraction development and ninety-degree phase shift is associated with the focusing.

show considerable diffraction development in association with the velocity pull-up or pull-down regions.

In these synthetic examples it is evident that effects due to transmission of waves through lenses are more complex phenomena than simple one-dimensional velocity pull-up or pull-down. Diffraction development, large amplitude variations, and considerable lateral displacement of reflector energy can all occur. Lateral velocity variations above a reflector can induce phantom structures that have no association with actual reflector geometry, and, perhaps more importantly, they can induce anomalous amplitude brightening or diminution that is not correlated at all with reflector-strength variation.
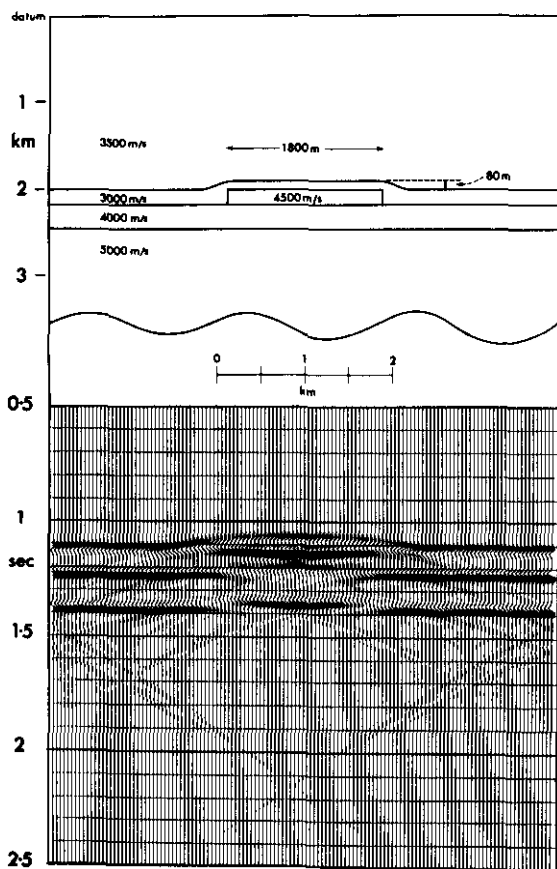

Fig. 5. Reef Model. The reef body acts to break up *reflections coming from lower reflectors. Note the existence of amplitude variations that have no correlation with reflector strength changes.*

Reefs are common exploration targets in the Alberta Plains. Illustrated in Figure 5 is a schematic composite reef model containing an abrupt change in velocity between onreef and offreef facies, and subtle drape on overlying sediments. The reef has an oblong shape and is composed of high-velocity carbonate material, surrounded and overlain by a shale unit of much lower acoustic impedance; both are situated on a platform of intermediate velocity. This arrangement produces several interesting effects in the resulting seismic data. The reef body acts to pull up reflections from the lower horizon in the region immediately beneath it, resulting in the break-up of the reflection into three parts. Because of the velocity arrangement of the reef, offreef and platform, the reflection from their contact undergoes a 180° phase shift between the reef-platform and offreef-platform portions of the reflection. This shift again results in the break-up of this reflection, and also causes the apparent thickness of the reef to be much less than that of the shale. Diffracted waves occur in association with all terminated reflections, and decay rapidly in amplitude. Diffraction development is many times swamped by noise or reduced in the stacking process (diffractions stack in at anomalously high velocities), so that their observation on real seismic data can be difficult. Sometimes diffraction presence is shown only by interference patterns.

In many regions, tectonic processes have brought about pronounced folding and faulting of rock layers. These geological conditions bring about not only complex reflector geometries, but also complex velocity gradients. Thus, *the processes of both reflection and refraction* come into play in actively causing distortions in reflection events.

The geology of the first structural example (Fig. 6) is analogous to that of the northwestern edge of the Green River basin in Wyoming, a slice of Precambrian rock thrust on top of flat-lying sedimentary strata. The Precambrian overthrust wedge acts as a huge divergent lens on reflections originating from lower strata, because of its higher velocity and the curvature of the mutual contacts. Reflections from strata beneath it have considerable horizontal and vertical displacements, and are completely separated from the unperturbed reflections from contiguous strata. Associated with this break-up are very pronounced diffraction de-
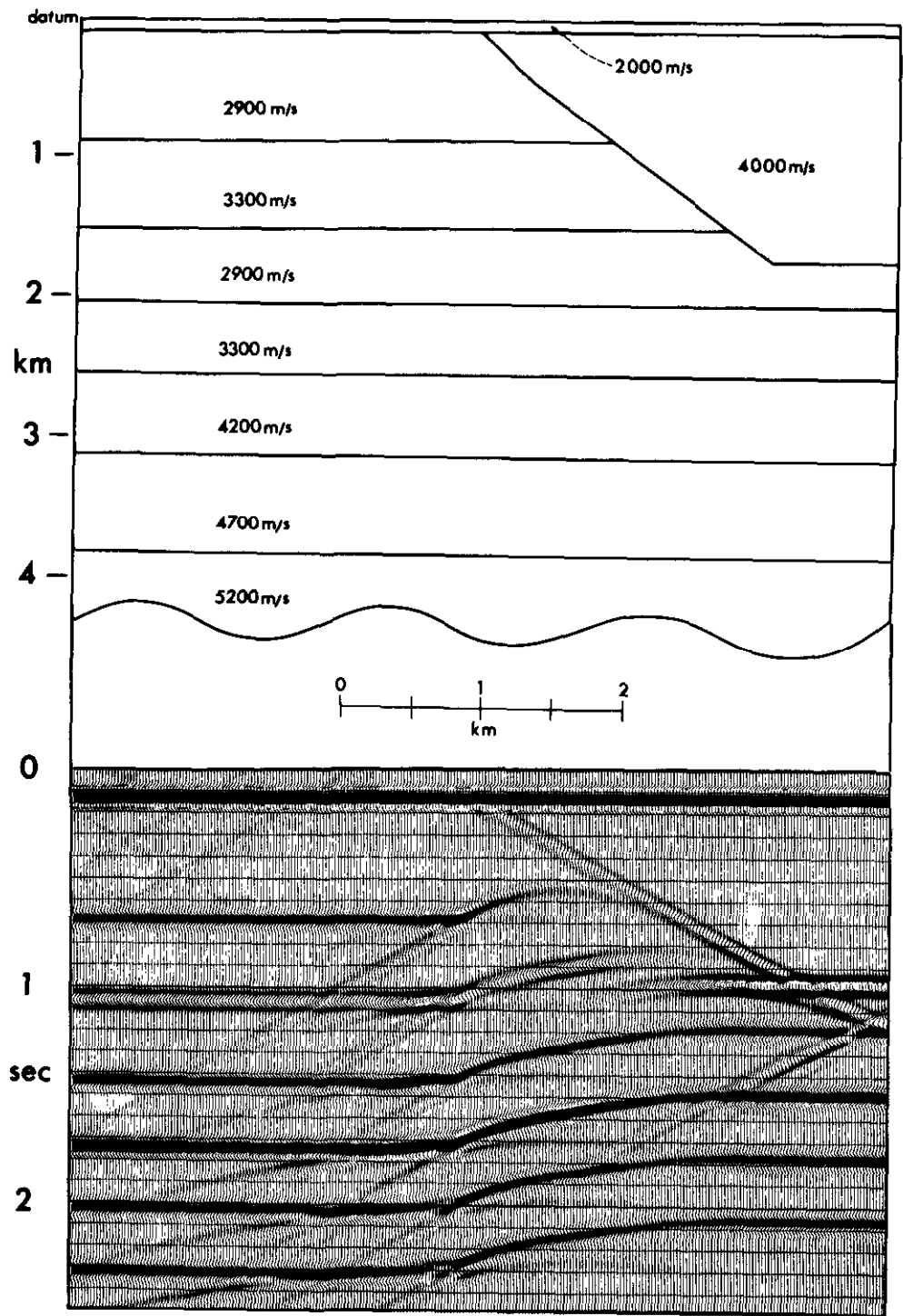
Fig. 6. Precambrian Overthrust. The wedge of Precambrian Strata acts to pull up and diverge reflections from the lower flat-lying strata.

velopments; these could be used as a tool in delineating the leading edge of the overthrust.

Note how the discontinuous change in velocity of the sedimentary units with depth affects the appearance of the pull-up zone: both a slight angularity in the shape of the event, and amplitude variations, are introduced even in regions a good distance from the 'leading edge' of the disturbance zone. Where the diffraction events meet the unperturbed reflection events, a fairly complex interference pattern emerges; with increasing depth, the pattern's complexity increases. All the features examined in the model data actually occur on real seismic data derived from this region, even though the stacking process does tend to distort the above-mentioned features further.
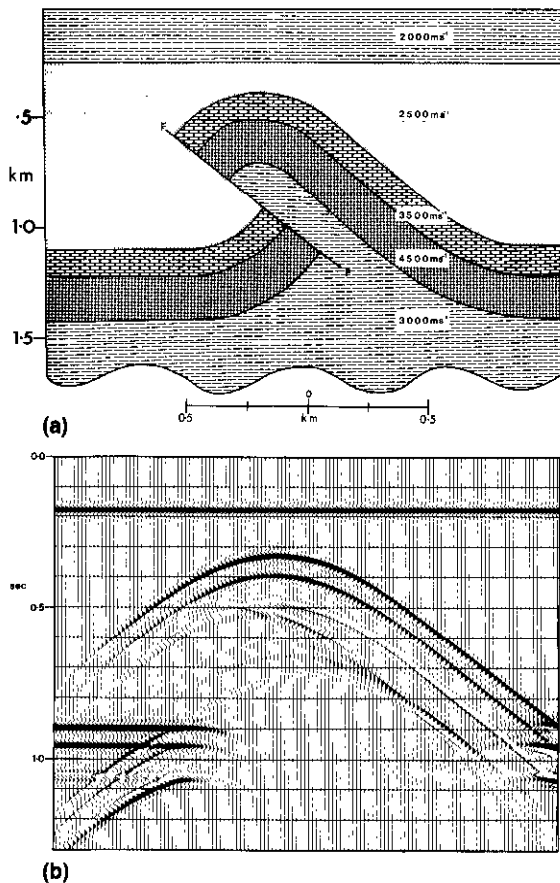

Fig. 7. Faulted Anticline. The upthrown side of the fault acts as both a focusing and an unfocusing lens on seismic data originating from the fault plane.
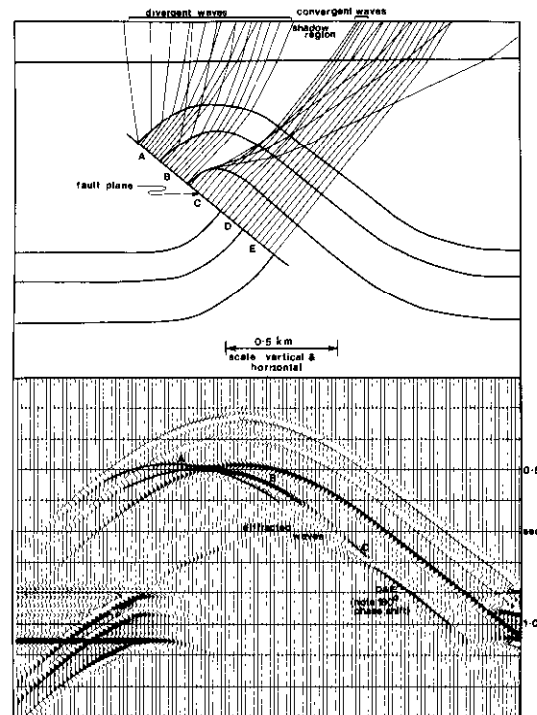

Fig. 8. Upper Diagram: Ray-tracing solution of the reflections from the fault plane, showing the properties of the lenses formed by the anticlinal structure. Lower Diagram: Location of the fault-plane reflections on the seismic model data. (Note display polarity opposite to Fig. 7.)

The second structural example (Fig. 7) is a faulted anticline. Basically, it consists of three layers of competent high-velocity materials faulted and folded within incompetent low-velocity materials. This example is included because, even through there are no obvious external lens-like objects, the structure itself acts to refract reflections originating from within it. Of interest to this study is the reflection originating from the fault plane. The fault plane can be subdivided into five elements (labelled A through E in Fig. 8), the distinction between them being the varying degrees of velocity contrast across the plane. Figure 8 has a partial ray-tracing solution of the reflection from the fault plane drawn on it for comparison and identification purposes.

As the figure shows, the curvature and greater velocity of the upper competent layers act as divergent lenses to waves emanating from the upper two fault-plane elements (A and B). The two reflections corresponding to these elements appear as broad, relatively low-amplitude

arcuate forms. They appear lower in amplitude, tilted and over a much broader region than if the processes of refraction were inoperative. The reflection from the third region of the fault plane encounters the folded strata as a convergent lens. Note that here the lens material is actually the incompetent low-velocity rock caught between the fault plane and the folded strata; this, along with the geometry of the contact between the incompetent material and the folded high-velocity material, ensures that the entire configuration acts as a focusing lens. Thus, in spite of the lower reflector strength of C, it appears in the record as a localized, relatively high-amplitude band. Note that the ray tracing in Figure 8 predicts the existence of a shadow zone between the reflections from elements B and C. The wave-theory solution shows this region to be filled with low-amplitude diffraction energy originating not only from the terminations of B and C, but also from portions of the curved surfaces situated on strata on the downthrown side of the fault. Reflections from the last two fault-plane elements (D and E) encounter no curved surfaces, so that no convergence or divergence of waves takes place.

Reflections from fault planes can be quite complex, appearing in any location depending on velocity configuration, but rarely in expected areas. The properties that determine whether a particular configuration acts as a convergent lens, divergent lens or neither —

that is, velocity contrast coupled with contact geometry — can change drastically over a relatively small region.

MODELING APPLICATION TO REAL DATA

Seismic data derived from the Alberta foothills region contain many of the features described previously in this paper. The tectonic style of deformation in this area is that of thrust faulting, whereby older Paleozoic rocks are thrust on top of younger Mesozoic strata.

Two seismic lines are presented. One is an older "100%" section, illustrated in Figure 9, and the other a multifold stack (Fig. 10). Seismic markers shown on both sections are reflections from the undisturbed Cambrian strata, and probably the top of the Mississippian. The tectonic thickening of the Paleozoic strata on the west end of both sections has produced a high-velocity divergent lens, resulting in perturbations on waves emanating from the Cambrian horizons. This perturbation shows up as a fault-like feature on the multifold line, and as a bow-tie-like feature complete with diffraction development on the 100% section. It should be noted that the 100% section has a much greater amount of diffraction energy criss-crossing the section than the multifold line has. This effect is probably due to the fact that diffracted waves do not obey the simple assumptions underlying CDP stacking and normal-moveout removal; diffractions stack in at anomalously high velocities, and thus tend to disappear on a CDP stack.
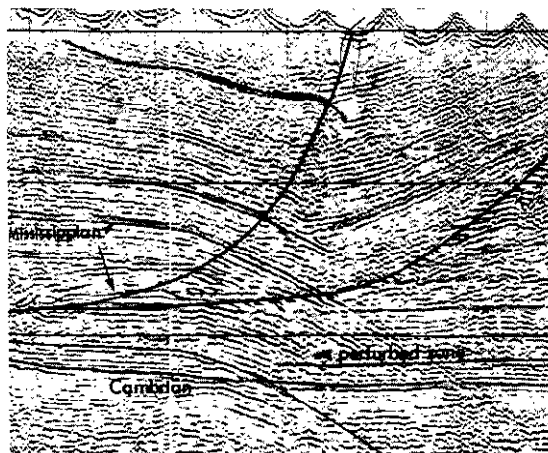

Fig. 9. 100% line from the Alberta Foothills. Tectonic thickening of the Paleozoic Strata in the west end of the section produces a divergent lens, causing perturbations on reflections from the Cambrian Horizons.
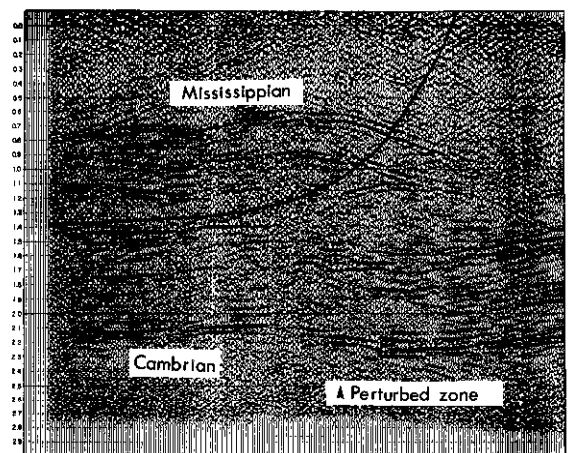

Fig. 10. Multifold line from the Alberta Foothills. Tectonic thickening of Paleozoic strata causes a fault-like feature in the Cambrian reflection where none actually exists.

To show that the above hypothesis of the origin of the structures on the Cambrian is at least plausible, the model shown in Figure 11 was devised. This model also illustrates the inherent ambiguity of seismic data. Note that the existence of the thrust labelled A on the geological model does serve to pull up and per- turb the reflection from the top of the "Cam- brian" in a manner similar to that shown in the real seismic data. On the reflection from the lower "Mississippian" horizon, two events, labelled B1 and B2, show up. The B1 event is actually a feature due solely to overlying later- al velocity changes caused by the presence of Thrust A. The B2 event is due to a legitimate structural feature, thrust B.

Because of the strongly laterally varying velocity fields present in the foothills, data de- rived from this region are not only difficult to interpret, but also difficult to process, since the reflections do not follow the stratified-earth assumptions implicit in modern multifold seis- mic processing. Velocities as deduced from the normal moveout present on data do not corres- pond in any meaningful way to actual RMS velocities; wave-equation migration fails to predict correctly the true position of the Cam- brian horizon, because the structural features seen on reflections from it do not originate at the same depth as the Cambrian itself, but at overlying depths.
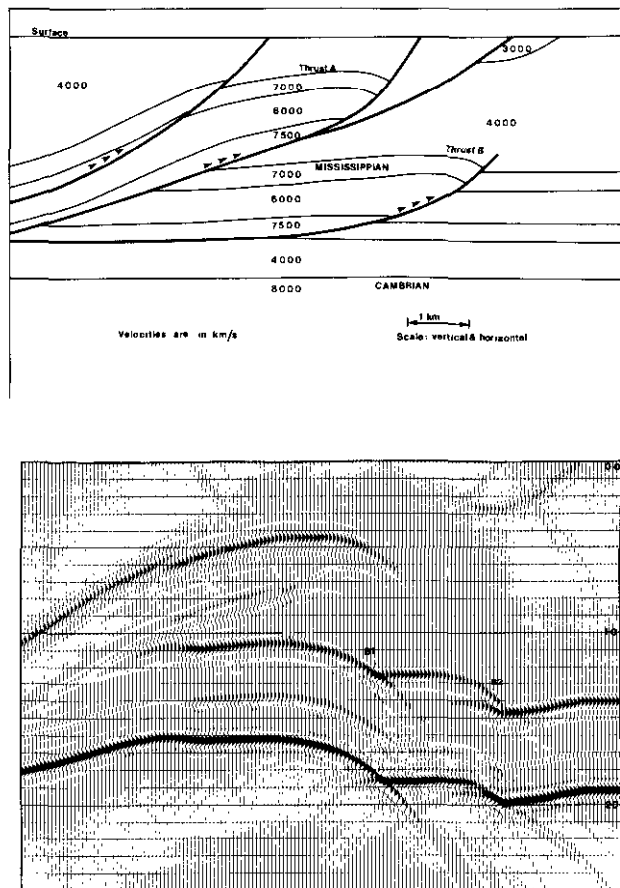

Fig. 11. Thrust Fault Model. Thrust fault A produces both a perturbation on the Cambrian reflection and one on the lower Mississippian reflection. This second feature closely resembles a legitimate feature produced by reflection from thrust fault B.

Conclusions

Several conclusions were reached during the researching and writing of this paper. The major ones are as follows:

1. The wave equation can be split into components that describe the propagation of both upcoming and downgoing wavefields, and the coupling between the two, in a manner that does not restrict the earth's subsurface to being either homogeneous or simply stratified.

2. For efficient wave-extrapolation algorithms, the operator that continues wavefields from one depth to another must be approximated optimally. The approximation given in equation 13 below is the most accurate expression for any given extrapolation distance; it becomes exact in the limit as lateral variations vanish, and in media with strong lateral inhomogeneities it remains accurate for wavefields of up to 45° dip.

$$e^{i\left\{\frac{\omega^2}{v^2|x|} + \frac{d^2}{dx^2}\right\}^{1/2}\Delta z} \cong e^{\left\{\{\psi_2^2 + \frac{d^2}{dx^2}\}^{1/2} + [\psi_{|x|} \; \psi] + O_{P_2}\right\}\Delta z} \quad (12)$$

$$\cong \left[e^{i\{\psi_2^2 + \frac{d^2}{dx^2}\}^{1/2}\Delta z} \right]\left[e^{i\{\frac{\omega}{v|x|} - \psi\}\Delta z} \right]\left[1 + O_{P_2} \; \Delta z \right]$$

$$O_{P_2} = \frac{1}{2}\left[\frac{v|x| - v}{\omega}\right]\frac{d^2}{dx^2} - \frac{1}{8}\left[\frac{v|x|^2 \; v^3}{\omega^3}\right]\frac{d^4}{dx^4} + \cdots \quad (13)$$

3. Lateral velocity variations can induce on a reflection event in seismic data all the features normally thought to result from the reflection process alone. They can create anomalous structures and amplitude variations that are not correlated in any way to corresponding reflector geometry or strength. As well, further distortions in reflections from complex regions where the reflection process alone would ensure large distortions in reflection events can

also occur. The seismic interpreter must be conscious of these effects. Care must always be taken to distinguish legitimate structures and legitimate amplitude variations from velocity-induced structures and amplitude variations.

References

Berkhout, A. J., 1980, New insight into forward modeling and migration: Presented at the Society of Exploration Geophysicists 50th Annual International Meeting, Houston.

Claerbout, J., 1971, Toward a unified theory of reflector mapping: Geophysics, v. 36, no. 3, p. 467-481.

———, 1976, Fundamentals of Geophysical Data Processing: New York, McGraw-Hill Book Co. Inc., McGraw-Hill International Series in the Earth Sciences.

Gantmakher, Feliks Ruvimovich., 1960, Matrix Theory, volume 2 (translated by K. A. Hirsh): New York, Chelsea Publishing Co.

Hilterman, Fred J., 1970, Three dimensional seismic modeling: Geophysics, v. 35, no. 6, p. 1020-1037.

Judson, D. R., Lin, J., Shultz, P. S. and Sherwood, J. W. C., 1980, Depth migration after stack: Geophysics, v. 45, no. 3, p. 361-375.

Larner, K., Gibson, B. and Diggons, C., 1980, Imaging beneath complex structure: a case history: Presented at the Society of Exploration Geophysicists 50th Annual International Meeting, Houston.

Loewenthal, D., Lu, L., Roberson, R. and Sherwood, J. W. C., 1976, The wave equation applied to migration: Geophysical Prospecting, v. 24, p. 380-399.

Longhurst, R. S., 1957, Geometrical and Physical Optics: London, Longman, Green and Co.

Tieman, H. J., 1980, Waves in Inhomogeneous Media: M.Sc. dissertation, University of Calgary, Calgary, Alberta.